Mat. Res. Soc. Symp. Proc. Vol. 729 © 2002 Materials Research Society

Nanogap Capacitors for Label Free DNA Analysis

Joon Sung Lee, Yang-Kyu Choi, Michael Pio, Jeonggi Seo and Luke P. Lee
Berkeley Sensor and Actuator Center
Department of Bioengineering, University of California at Berkeley, Berkeley, CA 94720

ABSTRACT

Nanogap capacitors are fabricated for DNA hybridization detection. Without labeling, the nanogap capacitors on a chip can function as DNA microarray sensors. The difference in dielectric properties between single-stranded DNA and double-stranded DNA permits use of capacitance measurements to detect hybridization. To obtain high detection sensitivity, a 50 nm gap capacitor was fabricated using a Si-nanotechnology. To ensure proper measurement of DNA's dielectrical properties, the probe ssDNA was first immobilized onto the electrode surface using self-assembly monolayers and allowed to hybridize with the target ssDNA. The capacitance changes were measured for 35-mer homonucleotides. The self-assembly monolayer and DNA immobilization events were verified independently by contact angle measurement and FTIR. Capacitance values are measured at frequencies ranging from 75 kHz to 5 MHz, using 0 V_{DC} bias and 25 mV_{AC} signals. Approximately 9% change in capacitance was observed after DNA hybridization at 75 kHz.

INTRODUCTION

Capacitance measurements can provide fast and sensitive *in-situ* monitoring of DNA hybridization without DNA labeling. This method provides an alternative to conventional DNA hybridization detection techniques such as radiochemical, enzymatic, fluorescent, and electrochemiluminescent methods, which can be cumbersome and time consuming processes because of the need for DNA labeling [1-3]. The investigation of dielectric properties of DNA was done even before the publication of Watson and Crick's double helix work, but it is not easy to implement in a DNA microarray system. Previously several groups have tried to measure DNA hybridization with capacitance measurement; however, their methods were limited in reproducibility and sensitivity [4, 5]. Berney *et al.* used an electrolyte-insulator-semiconductor scheme and obtained a 3% capacitance change but had trouble with reproducibility of the measurements due to the crudeness of the device [4]. Other researchers used an electrochemical method and observed a 2% capacitance change but also reported low reproducibility due to poor insulating properties of the oligonucleotide layer [5].

There are two different capacitance measurement methods. In the first method, the capacitance is measured at the solution-electrode interface with a three-electrode system. Using an appropriate circuit model, the capacitance can be calculated with measured current. In this method, the sensitivity variation in the bulk solution can be solved using a reference cell. However, only 2-3% capacitance changes were measured after hybridization and reproducibility issues were also reported [4, 5]. In the second scheme, DNA is placed in between two opposing electrodes and the capacitance change is measured. Their device is limited by the difficulty in reproducing narrow electrode gaps by mechanical means.

In this study, we report the first nanogap-based capacitors for the hybridization detection of DNA without labeling. Since it is difficult to attain nanoscale features with conventional photolithography, a novel spacer process technology is introduced to fabricate a 50 nm gap capacitor in between two electrodes with a 70mm length.

EXPERIMENTAL DETAILS:

Fabrication of Nanogap Capacitors

The steps involved in fabricating the DNA sensor are schematically illustrated in Fig. 1. One-side polished, <100> 4" silicon wafers are used as the starting material. Silicon nitride 0.6 μm, which serves as an etch stop in the final HF etch process and an insulator between two poly-Si electrodes and Si wafer, is deposited on the wafers by low pressure chemical vapor deposition (LPCVD).

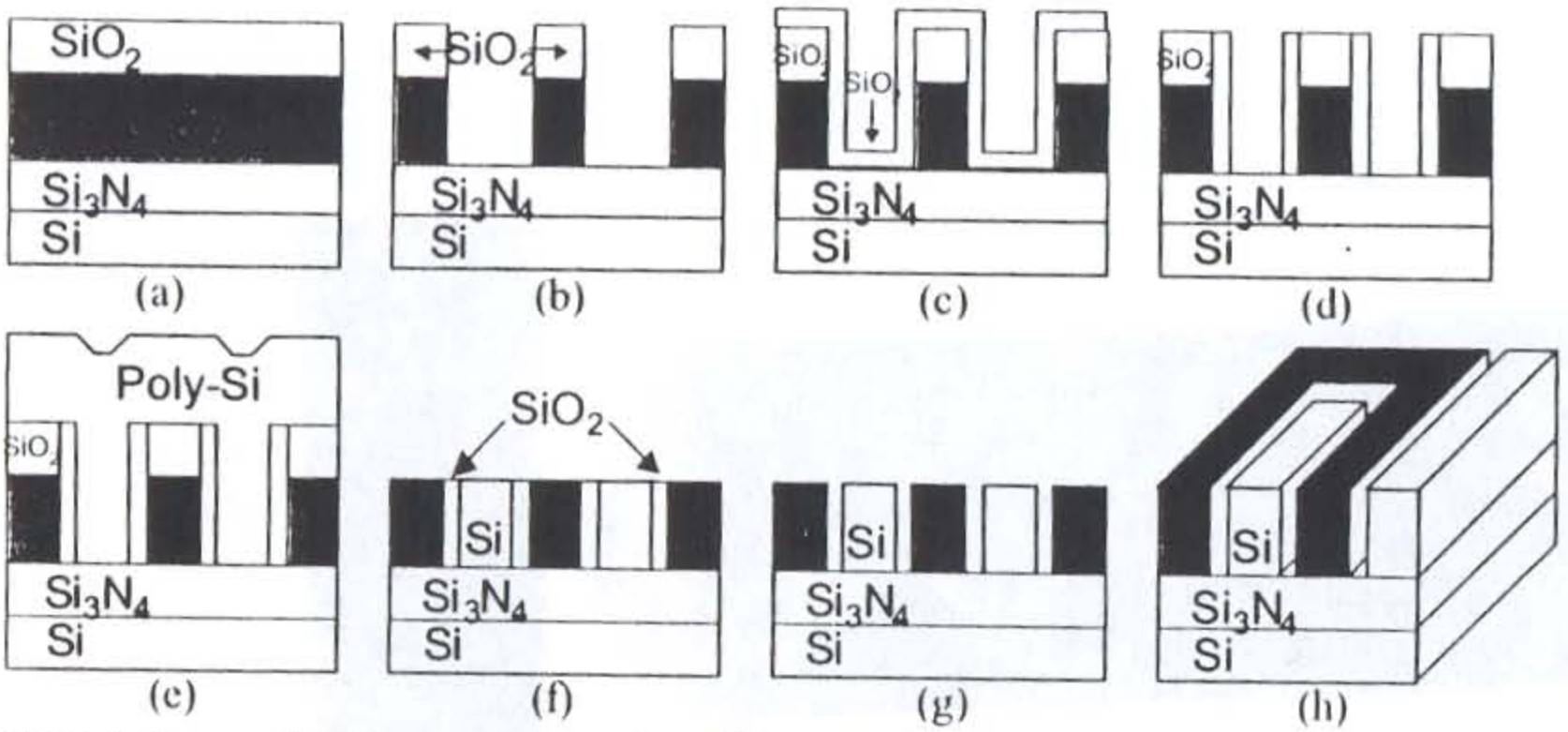

Figure 1. Process flow for a capacitance-based biosensor featuring 50 nm gaps: (a) SiO_2/poly-Si/Si_3N_4/Si, (b) pattern of SiO_2 and poly-Si with photolithography and etch of SiO_2 and poly-Si (c) deposit of SiO_2, (d) etch back oxide (e) deposition of poly-Si. (f) planarize by CMP, (g) etch away SiO_2 between two poly-Si layers and (h) 3-dimensional view of final device structure.

In-situ doped poly-Si (1 μm) which acts as an electrode (poly I), and 300nm of oxide are consecutively deposited, patterned with conventional photolithography and etched as shown in Fig. 1(b) in a Lam TCP 9400 etcher. The 300 nm of oxide acts as an etch stop in the chemical-mechanical polishing (CMP) step. Next, the photoresist is removed and 50 nm of oxide is deposited. In this process scheme, the minimum-sized gap is defined not by an optical lithography but by a deposited CVD film thickness. Thus, extremely narrow gaps beyond the limit of optical or e-beam lithography can be defined [6]. After oxide etch-back, 50 nm of oxide spacer is formed as shown in Fig. 1(d). 1μm of *in-situ* doped poly-Si (poly II) was deposited and the wafer was planarized by the CMP. Finally, the oxide spacers, which are between the two poly-Si structures, are etched away by HF. Fig. 1(h) shows 3-dimensional view of the final device structure. Due to the nonuniformity of CMP, 38% yield is obtained. This yield can be improved by optimization of CMP process. During capacitance measurements, the two poly-Si layers act as electrodes, so that the capacitance of DNA located between them can be measured.

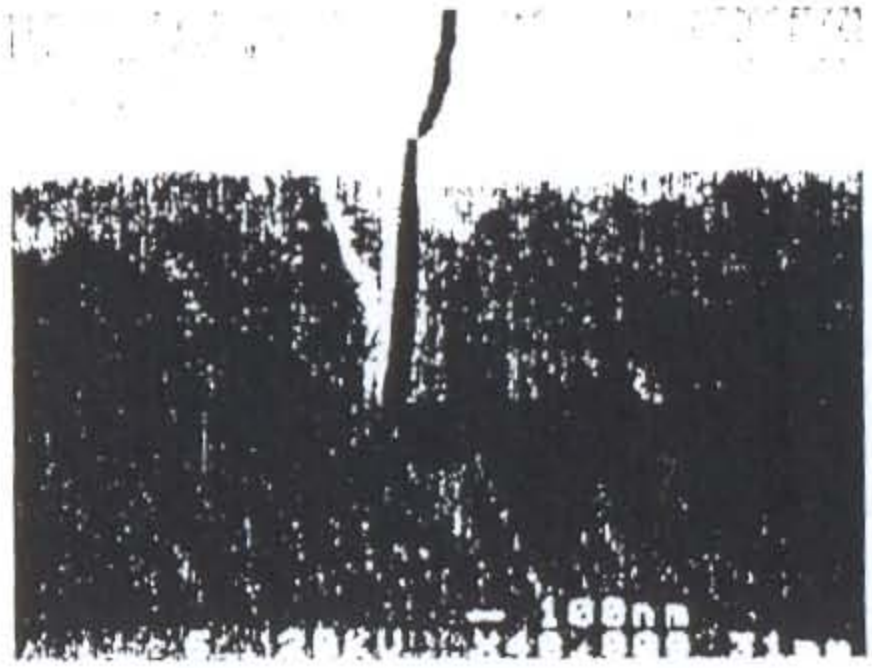

Figure 2. *Cross-sectional SEM view of a nanogap capacitor: There is a 50 nm gap between two electrodes.*

Figure 2 shows a cross-sectional SEM view of a device with 50 nm gap between two poly-Si electrodes. The 50 nm gap improves detection sensitivity and process window.

Immnobilization and Hybridization of DNA

Figure 3. *Procedure for preparation and characterization of capacitance-based DNA*

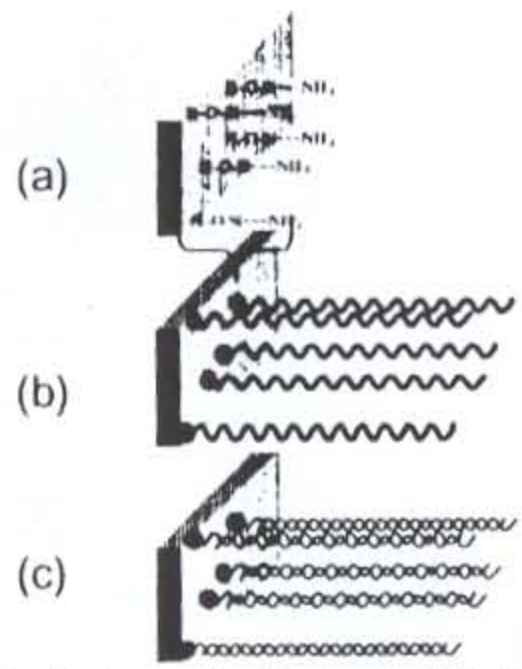

Figure 4. *A schematic diagram of (a) SAM- (b) immobilization- and (c) hybridization- treated Si surfaces.* ● *Represents SAM in (b) and (c).*

Table I Materials in experiment

Item	Description
SAM	(3-Aminopropyl)triethoxysilane
Solution for SAM	distilled deionized water
Poly T sequence (35mers)	5'-dTTTTT – TTTTT-3'
Buffer solution for immobilization	0.1mol/l N-methylimidazole buffer containing 0.1mol/l EDC (pH 6)
Washing solution in immobilization step	PBS
Poly A sequence (35mers)	5'-dAAAAA – AAAAA-3'
Poly G sequence (35mers)	5'-dGGGGG – GGGGG-3'
Buffer solution for hybridization	300mmol/l NaCl + 30mmol/l sodium citrate
Washing solution in hybridization step	PBS

RESULTS AND DISCUSSIONS

Figure 3 shows a procedure for sample preparation and characterization of DNA. Self-assembled monolayer (SAM) is applied to maximize the efficiency of hybridization. The materials used in this experiment are listed in Table I. To minimize the capacitance signal from the SAM, a short carbon-chain molecule is used. The devices are coated with a self-assembled monolayer of (3-aminopropyl)triethoxysilane (APS, Lancaster Co.). Solutions are diluted by mixing the APS with distilled-deionized (dd) water in a 100:1 ratio (v/v). The devices are immersed in the APS solution for 5 min and rinsed and dried with dd water and nitrogen, respectively [7]. 3-aminopropyl triethoxysilane has an amine group, which can be attached to the 5' end of ssDNA. Poly T 35-mer-homonucleotide is used for immobilization and 35-mer poly A and poly G probes are added to check hybridization events, which are complementary and noncomplementary DNA for poly T, respectively. The detail experimental procedure for immobilization and hybridization is described in previous report [8].

The SAM, DNA immobilization, and hybridization processes are verified separately by using contact angle measurements, Fourier Transform Infrared Spectroscopy (FTIR) and capacitance measurements. Contact angles of 2.5 μL of water droplets are measured and IR spectra are obtained at room temperature using a Genisis II FTIR and Drop Shape Analysis System DSA10, respectively. In contact angle measurement, a water contact angle is increased from $<30^{\circ}$ on SiO_2 to $>60^{\circ}$ on SAM-coated surfaces. This implies that the SAM process is successful. The capacitance is measured after monolayer formation, DNA immobilization, and DNA hybridization. At first, capacitance is measured after SAM treatment. Then, poly-T oligonucleotide is immobilized on the SAM treated poly-Si electrodes and are washed with PBS solution (8 g/L NaCl + 0.2 g/L KCl + 1.44 g/L Na_2HPO_4 + 0.2 g/L KH_2PO_4, pH 7.0). The device is dried with nitrogen and then the capacitance of the immobilized device is measured. For hybridization, poly A and poly G probes are added and are washed with PBS solution and are dried by nitrogen again. Finally, a change of capacitance by hybridization is measured. Figure 4 shows a schematic diagram of a device at the SAM, immobilization and hybridization steps. In fig. 4(b) the SAM is represented by black solid circle. The SAM on native oxide on poly-Si electrode, immobilized ssDNA on the SAM and dsDNA on the SAM are shown in Fig. 4(a), (b) and (c), respectively. In capacitance measurements, the permittivity and dielectric loss of DNA are investigated at frequencies between 75 Hz and 1 MHz, $0V_{DC}$ bias and 25 mV_{rc} signals using a HP4285A LCR meter. Generally, capacitance is a function of measurement frequency. To optimize the frequency for high detection sensitivity on DNA hybridization, the capacitances are measured at various frequencies. The concentrations of DNA are varied to determine the minimum detection limit for bioassays. Figure. 5 shows the FTIR spectrum of the SAM and immobilized DNA on a device in the range of 500~4000 cm^{-1}. The SAM and the immobilized DNA on SAM show a typical FTIR spectrum [9, 10]. The formation of a SAM coating with an $RSiCl_3$ precursor eventually produces covalent siloxane bonds, Si-O-Si. The absorption peak at 1100 cm^{-1} in Fig. 5(a) corresponds to the vibration of Si-O-Si. The absorption peaks at 3400 cm^{-1} and 2950 cm^{-1} in Fig. 5(a) correspond to the vibration of N-H and C-H, respectively. As shown in Fig. 5(b), immobilized DNA shows the stretching mode of the phosphate of the DNA fragments at 1080 cm^{-1} and the C-O stretching vibration of the base at 1700 cm^{-1} [8]. Based on these results, the processes for SAM and immobilization could be confirmed.

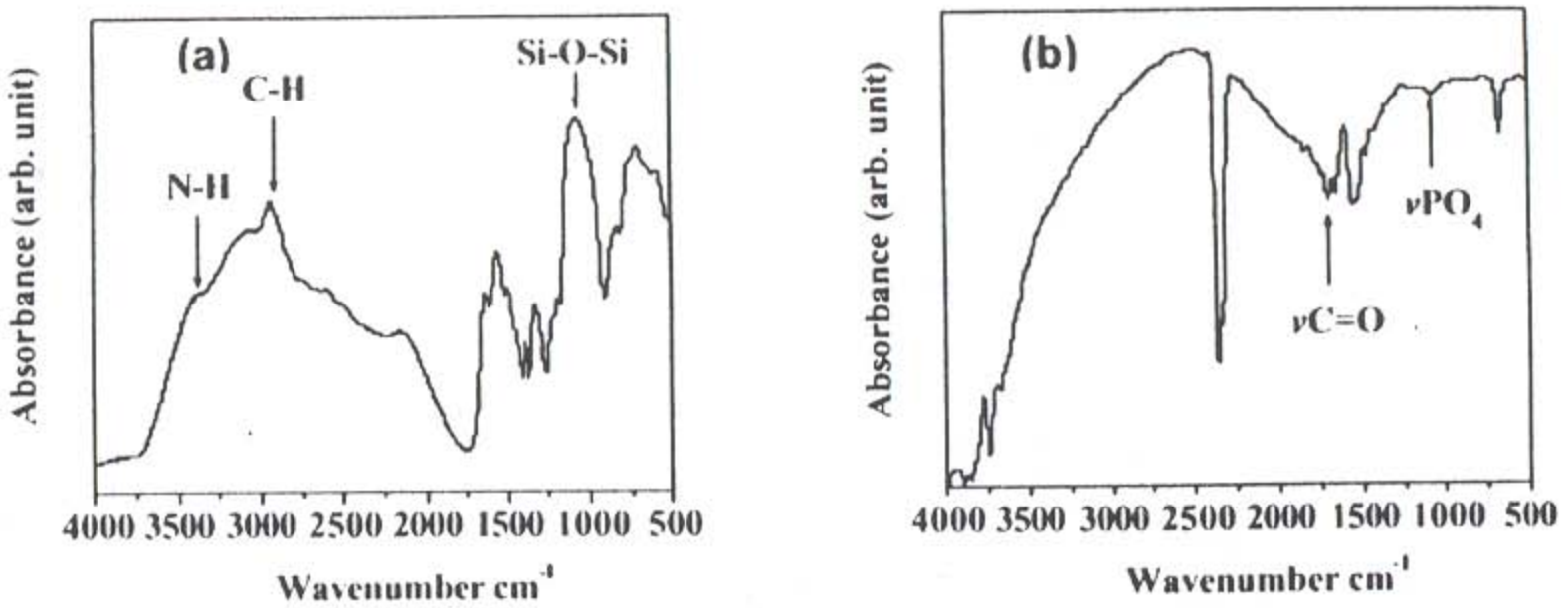

Figure 5. FTIR spectrum of differently treated surfaces such as (a) SAM on native oxide/poly Si surface and (b) ssDNA monolayer on SAM/native oxide/poly Si

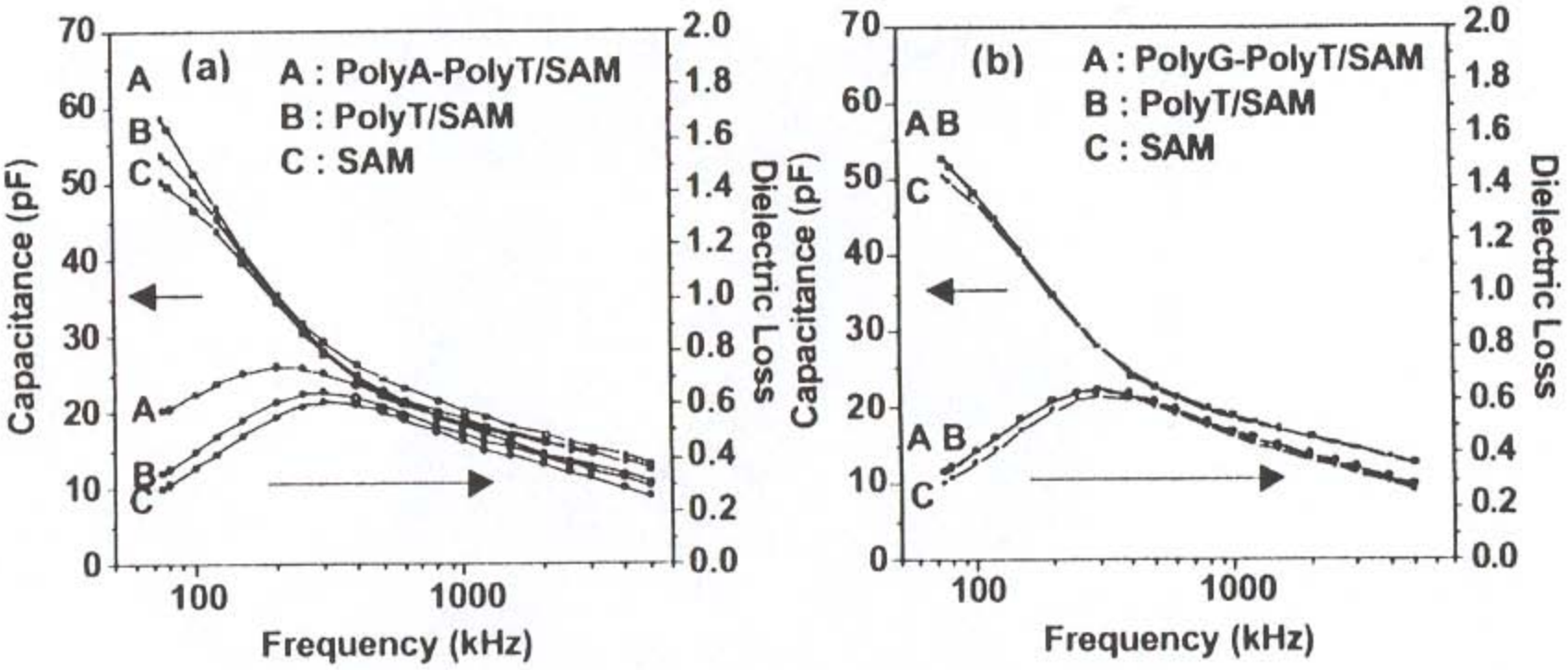

Figure 6. *Capacitance measurements with immobilization and hybridization at different frequencies using different polynucleotides (a) poly T and poly A and (b) poly T and poly G. The concentrations of poly T, poly A and ply G are 1x10^{-5} mol/L.*

Figure 6 shows the capacitance change with immobilization and hybridization with different homonucleotides at different frequencies. The capacitance increases as frequency decreases and 7-9% capacitance changes are observed at 75kHz in both immobilization and hybridization conditions in Fig. 6(a). Immobilization and hybridization increase capacitance due to the relatively higher dielectric constant of DNA as compared with air. To confirm the relationship between capacitance change and hybridization, a device with immobilized poly T is treated with poly G instead of poly A. Fig. 6(b) shows that there is no significant capacitance change between poly T and poly G. This results show that hybridization causes a capacitance change. Additionally, the DNA concentration dependency on capacitance change with hybridization is investigated (Fig. 7). For this experiment, we used 10^{-5} *mol/L* of Poly T at immobilization step and several concentrations from 10^{-7} to10^{-5} *mol/L* of Poly A were used at hybridization step. As conjugated DNA concentration is increased, capacitance change with hybridization is also increased. This data can also support the relationship between capacitance change and hybridization. But to get significant capacitance change, the required concentration of DNA should be in the micro molar range. In future work, device yield will be improved by either

optimization of CMP process or using a horizontal nanogap scheme instead of the current vertical nanogap scheme. In addition, low detection sensitivity will be improved by increasing electrode area, reducing the gap size, and operating at lower frequencies. However, further reducing gap size might introduce a sample plugging problem so additional agitation might be required.

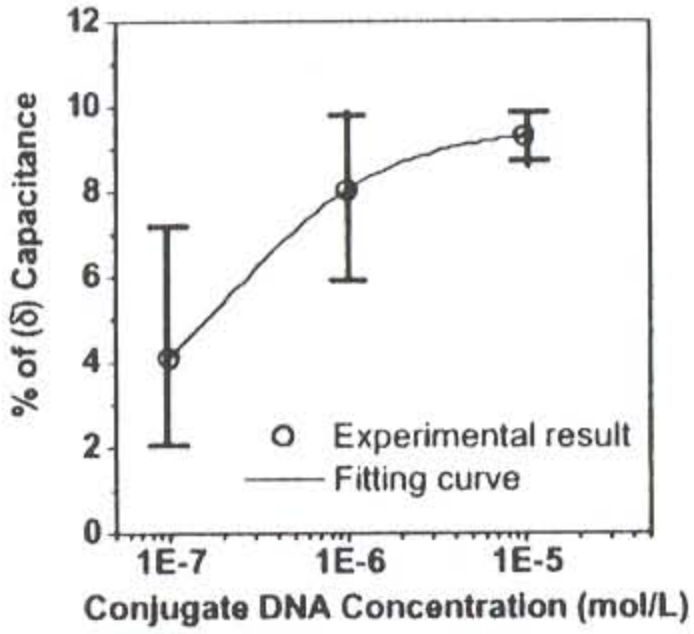

Figure 7. *Conjugate DNA concentration dependency on capacitance change with hybridization at 75kHz.*

CONCLUSIONS

The nanogap capacitors were designed, fabricated, and characterized for the detection of DNA hybridization. A capacitance-based biosensor, featuring vertical poly-Si/insulator/poly-Si and a 50nm gap, was prepared. To maximize hybridization efficiency, SAM and relatively short 35mer homonucleotides were used. The SAM and DNA immobilization were confirmed by FTIR and contact angle measurements. Higher capacitance changes were observed at lower frequency, around 75 kHz, resulting in 7-9 % increase in capacitance after DNA immobilization and hybridization. With the geometries of the current device, a higher sensitivity was obtained with a higher concentration of the target DNA in 0.1-10 micro *mol/L* ranges. However, this sensitivity can be improved by increasing the overall electrode area or by decreasing the gap between the two opposing electrodes as well as by operation in lower frequency ranges.

ACKNOWLEDGEMENTS

This work was partially supported by DARPA research program (JS), Department of Defense NDSEG Fellowship (MP), and a postdoctoral fellowship program (JL) from Korea Science and Engineering Foundation (KOSEF). The authors wish to thank Shahab Hadaegh, Kevin J. Yang, W. Robert Ashurst, and Wesley Chang for many key discussions.

REFERENCES

[1] G. Marrazza, I. Chianella, M. Mascini, *Biosensors and Bioelectronics* **14**, 43 (1999)
[2] E. Palecek, M. Fojta, M. Tomschik, J.Wang, *Biosensors and Bioelectronics* **13**, 621 (1998)
[3] P.A.E. Piunno, U.J.Krull, R.H.E. Hudson, M.J.Damah, H. Cohen, *Analytica Chimica Acta* **288**, 205 (1994)
[4] H. Berney, J. West, E. Haefele, J. Alderman, W. Lane and J.K.Collins, *Sensors and Actuators B* **68**, 100 (2000)
[5] C. Berggren, P. Stalhandske, J. Brundell and G. Johansson, *Electroanalysis* **11**, 156 (1999)
[6] Y.-K. Choi, T.-J. King, and C. Hu, *IEEE Trans. Electron Devices* **49**, 436 (2002)
[7] J. Hu, M. Wang, H. Weier, P.Frantz, W. Kolbe, D. Ogletree and M. Salmeron, *Langmuir* **12**, 1697 (1996)
[8] X. Sun, P. He, S. Liu, J. Ye and Y. Fang, *Talanta* **47**, 487 (1998)
[9] V.K. Rastogi, Chattar Singh, Vaibhav Jain and M. Alcolea Palafox, *J. Raman Spectrosc.* **31** 1005 (2000)
[10] Shuliang L. Zhang, Kirk H. Michaelian, and Glen R. Loppnow, *J. Phys. Chem.* A **102**, 461 (1998)